Mon. Not. R. Astron. Soc. **330,** 63–68 (2002)

Radio images of four luminous blue variable stars

R. A. Duncan[1★] and S. M. White[2]
[1]*Australia Telescope National Facility, PO Box 76, Epping NSW 2121, Australia*
[2]*Department of Astronomy, University of Maryland, College Park MD 20742, USA*

Accepted 2001 October 9. Received 2001 October 9; in original form 2001 June 27

ABSTRACT

We have used the Australia Telescope Compact Array to image four southern luminous blue variable stars: AG Car, He3-519, HR Car and WRA 751, at wavelengths of 3 and 6 cm, and resolutions of 1 and 2 arcsec respectively. With the partial exception of HR Car, all radio images show an unresolved stellar core surrounded by a large ionized gaseous nebula, and agree well with published Hα and [N II] optical images. The image of WRA 751 shows a stellar torus or disc. HR Car's radio image is unusual, and seems best explained by the presence of a hot binary companion.

Key words: circumstellar matter – stars: individual: AG Car – stars: individual: HR Car – stars: individual: He3-519 – stars: individual: WRA 751 – radio continuum: stars.

1 INTRODUCTION

Luminous blue variables (LBVs) are very massive stars that have evolved off the main sequence en route to becoming Wolf–Rayet stars (Maeder 1984, 1989; Humphreys 1989). They are characterized by large initial main-sequence masses ($\sim 50\,M_\odot$), large luminosities ($>10^5\,L_\odot$) and variable visual brightness. Episodically, at intervals of hundreds or thousands of years, they suffer major eruptions and eject several $M_\odot$ of material. The stage is short-lived, and as a consequence only about 10 LBVs are known in our galaxy, but two of them, η Carinae and P Cygni, are amongst the most famous of all stars.

The mass loss from LBVs during large outbursts may be greater than that for any other single stars except supernovae, and because of this and their enormous luminosity, they dramatically influence their environment. Infrared and optical observations have shown that six of the known galactic LBVs (η Carinae, AG Car, HR Car, He3-519, WRA 751, and HD 168625) are surrounded by dust and ionized gas (Hutsemékers 1994). This surrounding ionized gas should produce thermal emission at radio wavelengths, and indeed such emission has been found in the LBVs P Cygni (Wendker, Baars & Altenhhoff 1973; White & Becker 1982), HD 168625 (Leitherer, Chapman & Koribalski 1995), AG Car (Milne & Aller 1975), and detected and imaged from η Carinae (Retallack 1983; White et al. 1994; Duncan, White & Lim 1997; Duncan et al. 1999). G25.5 + 0.2, possibly an optically obscured LBV, has also been imaged at radio wavelengths (Cowan et al. 1989; Subrahmanyan et al. 1993). The aim of the work reported here has been to obtain radio images of the four hitherto unimaged southern LBVs, AG Car, He3-519, HR Car and WRA 751, all in the constellation Carina.

★E-mail: rduncan@atnf.csiro.au

2 OBSERVATIONS

The observations were made with the Australia Telescope Compact Array, at Narrabri New South Wales from 1994 to 1996, at two wavelengths, usually 3 and 6 cm, simultaneously. The most frequently used configuration comprised six 22 m antennas along an east-west array, such that the baselines were almost equally spaced from 337 to 5939 m (6 km array). At a wavelength of 3 cm, this configuration yields an angular resolution of about 1 arcsec, but is insensitive to structure larger than about 30 arcsec. Therefore, to provide information on possible larger-scale structure, these long-baseline observations were supplemented with observations at shorter spacings. In these short-baseline observations, the baselines were approximately equally spaced between either 153 and 1468 m (1.5 km array) or 77 and 735 m (0.75 km array). All observing sessions were approximately 12 hours in length, but this time was sometimes shared between two or more sources. In such cases, to obtain reasonable u–v coverage, the time on each source was split into about six sections, distributed over the Local Sidereal Time range of the source. Details of the observing dates, frequencies, and array lengths are given in Table 1.

3 ANALYSIS AND RESULTS

Images were obtained through the use of AIPS and MIRIAD software packages, and are shown in Figs 1 to 4. Although the observations yielded absolute positions (Table 2), the images shown in Figs 1 to 4 have all been centred on the radio position of the central star.

The radio images of all four LBVs show both compact stellar cores and extended ionized gaseous nebulae. These images were used to estimate stellar positions, and stellar and nebular fluxes and spectral indices.

Table 1. Observing parameters. Observing frequency is in MHz.

Date	Array length (km)	Frequency First	Frequency Second	Observing time (h) AG Car	HR Car	He3-519	WRA 751
94 Jan 29	6.0	5444	8873	9.4	–	–	–
94 Mar 6	0.75	5444	8873	11.6	–	–	–
94 Aug 23	6.0	5444	8585	–	2.1	2.1	2.1
94 Sep 5	6.0	5444	8585	–	1.1	–	–
95 Jan 2	6.0	5855	9200	–	10.7	–	–
95 Apr 11	6.0	8256	9024	–	11.3	–	–
95 May 28	1.5	5855	8256	1.4	8.7	–	–
95 Nov 9	6.0	5444	8585	1.4	1.4	–	–
95 Dec 9	6.0	5444	8585	1.4	1.4	–	–
96 May 19	0.75	5312	8576	–	–	5.3	5.1
96 May 20	0.75	5376	8626	1.9	–	4.0	3.9
96 Jul 18	6.0	5444	8585	–	–	1.6	1.6
Total				27.1	36.7	13.0	12.7

Table 2. Optical and radio positions of central stars.

Source	AG Car	He3-519	HR Car	WRA 751
RA (optical)	10:56:11.5839	10:53:59	10:22:53.8487	11:08:40.3
(radio)	10:56:11.59	10:53:59.58	10:22:53.87	11:08:40.07
Dec. (optical)	−60:27:12.872	−60:26:42	−59:37:28.398	−60:42:51
(radio)	−60:27:12.6	−60:26:44.3	−59:37:28.2	−60:42:51.6

Table 3. Stellar and nebular radio fluxes and Hα optical flux.

Source	AG Car	He3-519	HR Car	WRA 751
Stellar flux (6 cm) (mJy)	1.30	4.75	2.30	5.09
Stellar flux (3 cm) (mJy)	1.23	6.06	4.46	6.25
Stellar flux Spectral Index	−0.1	0.5	1.4	0.5
Nebular flux (6 cm) (mJy)	268.7	32.9	13.8	24.0
Nebular flux (3 cm) (mJy)	250.3	31.5	11.0	26.6
Nebular flux Spectral Index	−0.1	−0.1	−0.5	0.2
Hα flux (10^{-11} erg cm^{-2} s^{-1})	17.4	2.8	0.63	5.1

3.1 Stellar positions and fluxes

At both 3 and 6 cm, the positions and fluxes of the stellar cores were estimated by using the Gaussian-fitting AIPS utility IMFIT. The stellar flux estimates were then confirmed, and in some cases fine-tuned, by subtracting this flux as a model point source in the $u-v$ plane and checking that this indeed exactly removed the star from the image.

Table 2 lists, for all four stars, published optical positions, and radio positions obtained from the 3-cm images.

3.2 Nebular fluxes

Nebular fluxes were estimated from $u-v$ data from which the stars had been subtracted as described above. For each LBV, IMEAN was run to find the total flux in a rectangle tightly embracing its nebula. For a given LBV the same rectangle was used for both the 3- and 6-cm images.

Table 3 lists, for both the stellar and nebular components of each object, the 6- and 3-cm radio fluxes, and the spectral indices implied by these fluxes. Also shown are Hα fluxes measured by various observers and summarized by Hutsemékers (1994).

4 DISCUSSION

The spectral indices of the stellar component of all four LBVs (Table 3) suggest thermal emission. Although its weakness compared with the nebular flux probably limited measurement accuracy, both this weakness and the spectral index of AG Car's stellar emission are consistent with a weak optically thin wind.

The spectral indices for He3-519's and WRA 751's stellar emissions are both close to the value (0.6) to be expected from thermal emission in a spherically symmetric radially expanding stellar wind (Panagia & Felli 1975; Wright & Barlow 1975). We may therefore use the 3-cm fluxes given in Table 3 and the formula given by Wright & Barlow (1975) to estimate the mass-loss rates of these two stars. For He3-519 we shall adopt a distance (D) of 8 kpc, and a terminal wind velocity of 365 km s^{-1} (Hutsemékers 1994; Davidson et al. 1993; Smith, Crowther & Prinja 1994), and for WRA 751 a distance (D) of 7 kpc, and a terminal wind velocity of 175 km s^{-1} (Hutsemekers & Van Drom 1991b; Hu et al.1990;

Van Genderen et al. 1992; Garcia-Lario, Riera & Manchado 1998). We shall adopt, as appropriate for LBVs, electron temperatures at the radio photosphere of $T_e = 12\,000$ K, and the molecular and ionic composition parameters $\mu = 1.5$ and $Z = \gamma = 1.0$. We thus derive from Wright & Barlow's formula mass loss rates of $1.2 \times 10^{-4}\,M_{\odot}\,yr^{-1}$ for He3-519, and $5.0 \times 10^{-5}\,M_{\odot}\,yr^{-1}$ for WRA 751.

HR Car's larger stellar spectral index (1.4) is consistent with a wind having an ion density that, probably because of recombination, falls off with distance from the star (r) more rapidly than r^{-2} (Olnon 1975; Panagia & Felli 1975; Wright & Barlow 1975).

The near-zero spectral indices of the nebular component of three of the LBVs, AG Car, He3-519 and WRA 751, are consistent with optically thin thermal emission (Mezger, Schraml & Terzian 1967), but HR Car's markedly negative nebular spectral index suggests non-thermal emission (Table 3).

We will now describe and discuss in detail the images of each of the four sources. AG Car, He3-519 and WRA 751's 3- and 6-cm images are similar, and for this reason only 3-cm images, which have the better resolution, are shown. However, HR Car's 3- and 6-cm images differ, and for this reason both are shown. The images of AG Car and He3-519 hold few surprises, but those of WRA 751 and HR Car are unusual and will be discussed in more detail.

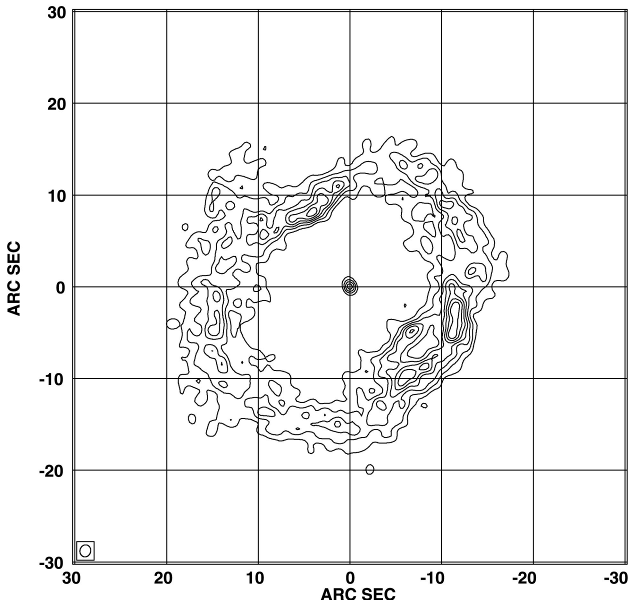

Figure 1. 3-cm wavelength radio image of AG Carinae. The lowest contour and the contour interval are 0.15 mJy arcsec^{-2}.

4.1 AG Car

Thackeray (1950) and Nota et al. (1992) have shown that AG Car is surrounded by a ring-like Hα and [N II] emission nebula. Fig. 1 shows AG Car's 3-cm wavelength radio image; we see that the nebula around AG Car appears to be a detached ring, with negligible gas close to the star. This radio image resembles in detail optical Hα and [N II] images of AG Car, and this not only confirms that the radio emission arises as optically thin thermal bremsstrahlung, but shows also that optical extinction over the image is remarkably uniform. Almost certainly this means that dust is negligible; McGregor et al. (1988) reached the same conclusion from 50-μm and 100-μm infrared observations.

4.2 He3-519

He3-519's 3-cm wavelength radio image is shown in Fig. 2, and has the same shape and diameter (55 arcsec) as the corresponding Hα image (Stahl 1987). It resembles AG Car in showing a stellar core surrounded by an ionized gaseous nebula, but differs in that its nebula appears to be a bubble rather than a detached ring. The radio image suggests that the gas is clumpy.

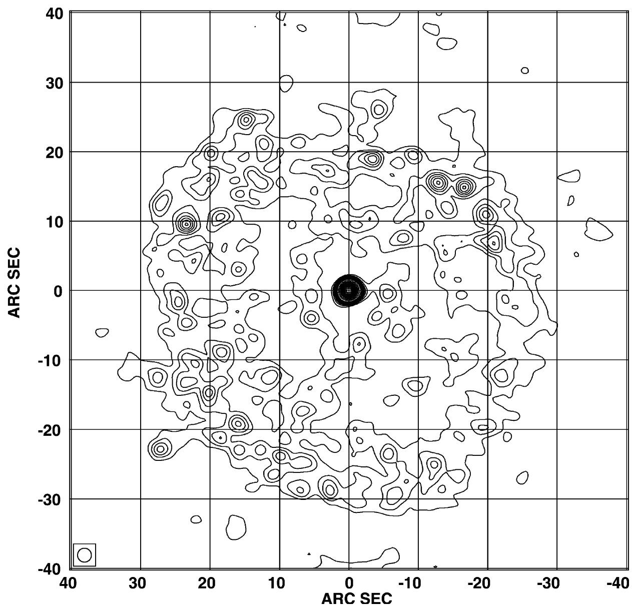

Figure 2. 3-cm wavelength image of He3-519. The lowest contour level is 0.01 mJy arcsec^{-2} and the contour interval 0.02 mJy arcsec^{-2}.

4.3 WRA 751

Optical Hα and [N II] images of WRA 751 show a roughly circular centrally concentrated nebula 22 arcsec in diameter (Hutsemékers & Van Drom 1991b). The radio images (Fig. 3) are very similar to the optical image, and show an almost attached nebula embracing a bright central star.

Subtraction of the central star as a point source in the u–v plane, as we routinely did for all LBV images, reveals a two-component structure which we interpret as a disc or torus around the central star; with hindsight, one can see it peeking out even in the unsubtracted image. This was the only LBV for which residual emission was left after subtraction of a model point source. Hutsemékers & Van Drom (1991b) and Garcia-Lario et al. (1998) almost certainly detected this torus optically; their studies of the forbidden nebular [N II] emission suggested that the star was tightly cocooned by nebular gas.

WRA 751's nebula is brighter on its north-east side than its south-west one, and this brightness gradient occurs even across the torus. The almost perfect morphological symmetry of the nebula would seem to exclude explanations in terms of interstellar winds or density gradients. However, η Carinae's nebula shows a similar asymmetry, and in that case it is known that the cause lies in ultraviolet illumination by a small hot companion star (Duncan et al. 1999). Perhaps WRA 751's nebula is illuminated by a small hot star to the north-east. The torus, also, is consistent with a companion star and consequent mass transfer.

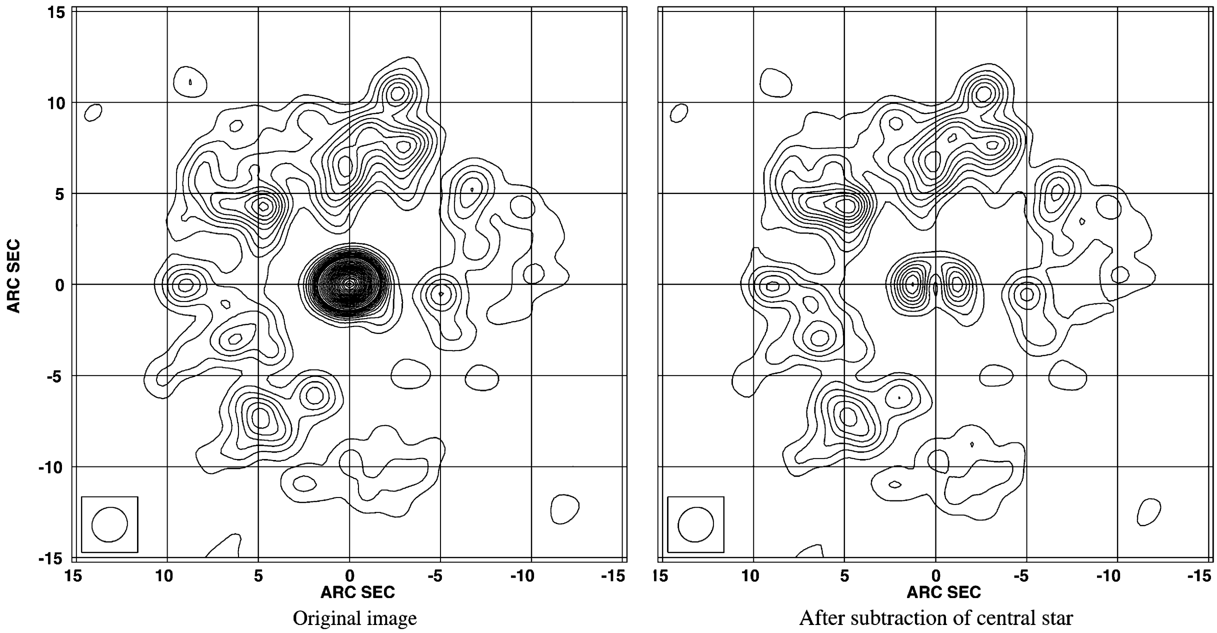

Figure 3. 3-cm wavelength images of WRA 751. Left panel: original image; right panel: after subtraction of central star. The lowest contour and the contour interval are 0.03 mJy arcsec^{-2}.

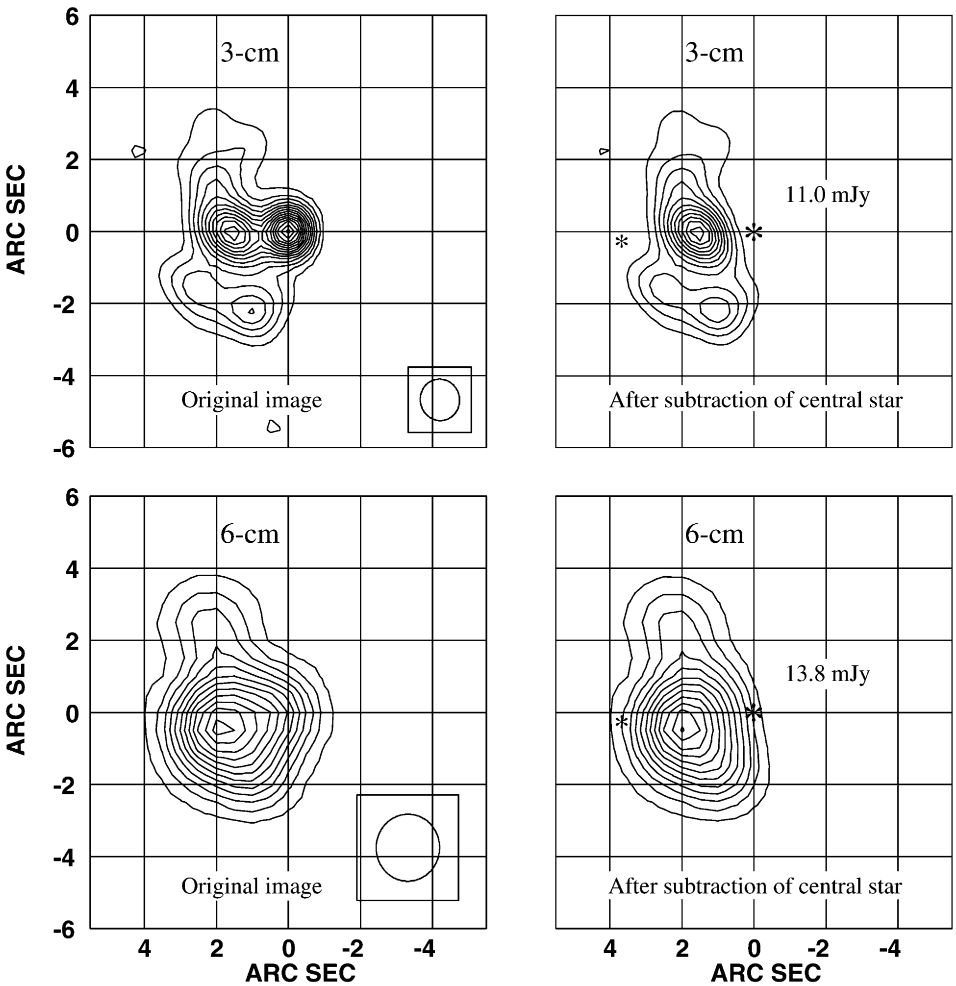

Figure 4. 3- and 6-cm wavelength images of HR Carinae both before and after subtraction of the central star.

4.4 HR Car

Hutsemékers & Van Drom (1991a) and Clampin et al. (1995) have shown that HR Car is surrounded by a centrally concentrated optical nebula. The most recent Hα optical image of HR Car is that of Nota et al. (1997). This shows a bright central north–south elongated core, surrounded by two, presumably polar, bubbles, with a total extent of 38 arcsec. Although the south-west bubble is the brighter, both bubbles are faint. The bubbles are faint at radio wavelengths also, but White (2000) has found correspondence between the radio and optical images.

In this paper we concentrate on the bright, well-detected, radio core. Fig. 4 shows images of this region at wavelengths of both 3 and 6 cm. The 3-cm image shows a strong component at the optical position of the star (*Hipparcos* Catalogue 1997; Table 2), and this almost certainly arises from a stellar wind immediately surrounding the star. The 3-cm image shows also a nebula to the east. The 6-cm image is dominated by this eastern nebula, and in it the contribution from the star appears only as a wide bulge.

Apart from the difference in the size of the beams, the reason for the difference between the 3- and 6-cm images is that the star has a positive (thermal) spectral index and thus dominates the 3-cm image, whereas the nebula has a negative (non-thermal) spectral index and thus dominates the 6-cm image (Table 3).

We are most interested in the nebula and to study this and properly compare the 3- and 6-cm images we must first subtract the star. In the case of the 3-cm image this is straightforward, but in the case of the 6-cm image one might doubt that it was possible; partly because of the large beam, the contribution from the star is poorly resolved, and appears only as a wide bulge. However in practice the standard procedure worked well on the 6-cm image; within limits, no matter what position was suggested to IMFIT as its initial guess, it homed in on the optical position of the star. Of course, that IMFIT finds the true position of the star does not prove that it finds the true flux, but it gives one a little confidence, and we have subtracted its estimate from the raw 6-cm data. Fig. 4 (right) shows the subtracted images, and we believe that these represent the nebula. We have determined the flux for both the 3- and 6-cm nebular images, and these fluxes (shown in both Fig. 4 and Table 3) show that the nebular emission is non-thermal.

The rms errors of these flux determinations, as calculated in the standard way from the rms noise in an area outside the source, are small, 0.1 mJy or less, but such calculations are a little academic as larger uncertainty is associated with the choice of box judged to embrace the nebula snugly. This latter uncertainty is difficult to evaluate analytically, but even if obviously over- or undersized boxes are chosen, the spectral index remains strongly negative.

A striking feature of Fig. 4 is the eastward displacement of the nebula from the primary star. At first sight this might suggest westward motion of the star relative to the interstellar medium, but the symmetry of the outer (double-bubble) optical nebula (Clampin et al. 1995; Nota et al. 1997) makes this explanation untenable. Another possibility might be that ultra-violet illumination from a hot star to the east ionizes gas on the eastern side of HR Car. This could explain, in the faint outer nebula, the greater optical brightness of the south-east bubble versus the northwest one. However we favour another explanation of the eastern displacement of the inner nebula.

The *Hipparcos* Catalogue (1997) lists HR Car as a suspected double, and Hutsemékers & Van Drom (1991a) and Weis et al. (1997) have noted the presence of a visual companion 3.7 arcsec to the east. We tentatively assume this eastern star to be the suspected binary companion, and in Fig. 4 mark both its and HR Car's positions with asterisks. It is evident that the nebula lies between these two stars with its major axis normal to their joining line. In the 6-cm image the nebula appears to overlap the stars but this appearance arises from the large 6-cm beam. Indeed even in the 3-cm image the nebula's half-power width is only 1.9 times that of the beam, and hence its width is barely resolved and probably narrower than Fig. 4 suggests. White (2000) discussed the possibility that the nebula might arise from the colliding winds of the stars, but concluded that this was unlikely. We however believe it likely; the position, shape, orientation, and non-thermal radio spectrum of the inner nebula all suggest the collision of the stellar winds of the two stars.

5 SUMMARY

The radio images of all four luminous blue variables (LBVs) and their surrounding nebulae closely resemble in size and morphology corresponding optical Hα and [N II] images.

Two of the LBVs show evidence of hot binary companions. WRA 751's nebula shows a north-east–south-west brightness gradient suggesting illumination by a hot companion to the north-east, and also a torus surrounding the central star, possibly suggesting mass transfer from a companion. HR Car shows a long thin nebula lying approximately midway between it and a visual companion, with the nebula's major axis normal to the joining line of the stars. We conclude that this nebula marks the collision shock of the stellar winds of the stars. The well-known LBV η Carinae is also known to have a hot binary companion (Duncan et al. 1999).

Indeed we would expect a high proportion of LBVs to have hot companions, because the more numerous Wolf–Rayet stars, which lie on the same evolutionary path, frequently have such companions. Williams et al. (1990, 1997) first found Wolf–Rayet systems with colliding winds. Chapman et al. (1999) found that 40 per cent of Wolf–Rayet stars with measured radio spectra had non-thermal spectra suggesting wind collision. Van der Hucht (2001) found that of 227 Wolf–Rayet stars studied, 39 per cent were binaries, and of these binaries 90 per cent of the companions were of class OB.

ACKNOWLEDGMENTS

We thank Dr Lister Staveley-Smith for encouragement, and our referees, Drs Mike Barlow, Jessica Chapman and Claus Leitherer, for careful reading of the manuscript and many helpful suggestions and comments.

REFERENCES

Chapman J. M., Leitherer C., Koribalski B., Bouter R., Storey M., 1999, ApJ, 518, 890
Clampin M., Schulte-Ladbeck R. E., Nota A., Robberto M., Paresce F., Clayton G. C., 1995, AJ, 110, 251
Cowan J. J., Ekers R. D., Goss W. M., Sramek R. A., Roberts D. A., Branch D., 1989, MNRAS, 241, 613
Davidson K., Humphreys R. M., Hajian A., Terzian Y., 1993, ApJ, 411, 336
Duncan R. A., White S. M., Lim J., 1997, MNRAS, 290, 680
Duncan R. A., White S. M., Reynolds J. E., Lim J., 1999, in Morse J. A., Humphreys R. M., Damineli A., eds, ASP Conf. Ser. Vol. 179, Eta Carinae at the Millennium. Astron. Soc. Pac., San Francisco, p. 54
Garcia-Lario P., Riera A., Manchado A., 1998, A&A, 334, 1007
Hipparcos & Tycho Catalogues, 1997, ESA Publications Division, Noordwijk

Hu J. Y., de Winter D., Thé P. S., Perez M. R., 1990, A&A, 227, L17
Humphreys R. M., 1989, in Davidson K., Moffat A. F. J., Lamers H. J. G. L. M., eds, IAU Colloq. 113, Physics of Luminous Blue Variables. Kluwer, Dordrecht, p. 3
Hutsemékers D., 1994, A&A, 281, L81
Hutsemékers D., Van Drom E., 1991a, A&A, 248, 141
Hutsemékers D., Van Drom E., 1991b, A&A, 251, 620
Leitherer C., Chapman J. M., Koribalski B., 1995, ApJ, 450, 289
McGregor P. J., Findlayson K., Hyland A. R., Marshall J., Harvey P. M., Lester D. F., 1988, ApJ, 329, 874
Maeder A., 1984, in Maeder A., Renzini A., eds, Proc. IAU Symp. 105, Observational Tests of the Stellar Evolution Theory. Reidel, Dordrecht, p. 299
Maeder A., 1989, in Davidson K., Moffat A. F., Lamers H. J. G. L. M., eds, IAU Colloq. 113, Physics of Luminous Blue Variables. Kluwer, Dordrecht, p. 15
Mezger P. G., Schraml J., Terzian Y., 1967, ApJ, 150, 807
Milne D. K., Aller L. H., 1975, A&A, 38, 183
Nota A., Leitherer C., Clampin M., Greenfield P., Golimowski D. A., 1992, ApJ, 398, 621
Nota A., Smith L., Pasquall A., Clampin M., Stroud M., 1997, ApJ, 486, 338
Olnon F. M., 1975, A&A, 39, 217
Panagia N., Felli M., 1975, A&A, 39, 1
Retallack D. S., 1983, MNRAS, 204, 669
Smith L. J., Crowther P. A., Prinja R. K., 1994, A&A, 281, 833
Stahl O., 1987, A&A, 182, 229
Subrahmanyan R., Ekers R. D., Wilson W. E., Goss W. M., Allen D. A., 1993, MNRAS, 263, 868
Thackeray A. D., 1950, MNRAS, 110, 526
van der Hucht K. A., 2001, New Astron. Rev., 45, 135
van Genderen A. M., Thé P. S., de Winter D., Hollander A., de Jong P. J., van den Bosch F. C., Kolkman O. M., Verhagen M. A. W., 1992, A&A, 258, 316
Weis K., Duschl W. J., Bomans D. J., Chu Y.-H., Jones M. D., 1997, A&A, 320, 568
Wendker H. J., Baars J. W. M., Altenhoff W. J., 1973, Nature Phys. Sci., 245, 118
White R. L., Becker R. H., 1982, ApJ, 262, 657
White S. M., 2000, ApJ, 539, 851
White S. M., Duncan R. A., Lim J., Nelson G. J., Drake S. A., Kundu M. R., 1994, ApJ, 429, 380
Williams P. M., van der Hucht K. A., Pollock A. M. T., Florkowski D. R., van der Woerd H., Wamsteker W. M., 1990, MNRAS, 243, 662
Williams P. M., Dougherty S. M., Davis R. J., van der Hucht K. A., Bode M. F., Setia Gunawan D. Y. A., 1997, MNRAS, 289, 10
Wright A. E., Barlow M. J., 1975, MNRAS, 170, 41

This paper has been typeset from a TEX/LATEX file prepared by the author.